



**Influence of the Ptolemy-Pliny-Strabo Fault Zone in Bozburun Peninsula
(Southwest Türkiye): Evidence from Structural Data and Focal Mechanism Solutions**
*Ptolemy-Pliny-Strabo Fay Zonu'nun Bozburun Yarımadası'ndaki (Güneybatı Türkiye) Etkisi:
Yapısal Verilerden ve Odak Mekanizma Çözümlerinden Elde Edilen Kanıtlar*

**Gürol Seyitoğlu^{1*}, Bülent Kaypak², Edanur Tanülkü³,
Tolga Karabıykoğlu², Begüm Koca²**

¹ Department of Geological Engineering, Tectonics Research Group, Ankara University, Ankara, Türkiye

² Department of Geophysical Engineering, Ankara University, Ankara, Türkiye

³ Institute of Earth and Marine Sciences, Gebze Technical University, Kocaeli, Türkiye

• Geliş/Received: 11.08.2023

• Düzeltilmiş Metin Geliş/Revised Manuscript Received: 04.10.2023

• Kabul/Accepted: 12.10.2023

• Çevrimiçi Yayın/Available online: 05.12.2023

• Baskı/Printed: 30.01.2024

Araştırma Makalesi/Research Article

Türkiye Jeol. Bül. / Geol. Bull. Turkey

Abstract: Structural data obtained from fault surfaces in the Bozburun Peninsula, southwest Türkiye indicate that the previously known active normal faults are indeed strike-slip structures. The configuration of left- and right-lateral strike-slip segments and lineaments observed from high-resolution satellite images, plus the evaluation of available focal mechanism solutions of the earthquakes having less than 30 km depth around Bozburun Peninsula, show that the study area is under influence of the left-lateral Ptolemy-Pliny-Strabo Fault Zone.

Keywords: Aegean Arc, Bozburun Peninsula, Ptolemy-Pliny-Strabo Fault Zone, Southwest Türkiye.

Öz: Güneybatı Türkiye'deki Bozburun Yarımadası'nda fay düzlemlerinden elde edilen yapısal veriler, daha önce bilinen diri normal fayların aslında doğrultu atımlı faylar olduğunu ortaya çıkarmıştır. Sol ve sağ yanallı doğrultu atımlı segmentlerin ve yüksek çözünürlüklü uydu görüntülerinden saptanan çizgiselliklerin dağılımı ve Bozburun Yarımadası çevresinde 30 km'den daha sığ depremlerin odak mekanizması çözümlerinin birlikte değerlendirilmesi, çalışma alanının sol yanallı Ptolemy-Pliny-Strabo Fay Zonu etkisinde olduğunu göstermektedir.

Anahtar Kelimeler: Bozburun Yarımadası, Ege Yayı, Güneybatı Türkiye, Ptolemy-Pliny-Strabo Fay Zonu.

INTRODUCTION

The Aegean Arc is one of the major neotectonic elements in the Eastern Mediterranean which was recognized in the initial years of plate tectonics theory (McKenzie, 1970; 1972; Papazachos and Comninakis, 1971; Dewey et al., 1973). The kinematics obtained from focal mechanisms of the earthquakes along the arc indicate that the eastern margin has a trench parallel strike-slip nature (Le Pichon and Angelier, 1979; Taymaz et al., 1990).

Today, the eastern margin of the Aegean Arc is known as the Ptolemy-Pliny-Strabo Fault Zone (PPSFZ) (Shaw and Jackson, 2010; Özbakır et al., 2013). Its left lateral strike-slip nature is also confirmed by the GPS data (Reilinger et al., 2006; 2010, i.e., 49.5±0.4 mm/year; Seyitoğlu et al., 2022a, i.e., 37.3±0.4 mm/year) and is attributed to the surface expression of active tearing on the subducting African slab reflecting typical Riedel and anti-Riedel fractures (Özbakır et al., 2013).

One of the major tectonic problems in the region concerns the continuation of the PPSFZ into the mainland of Türkiye as the Fethiye-Burdur Fault Zone (FBFZ). There are two different arguments. The first group of researchers is in favour of the FBFZ (Barka and Reilinger, 1997; Ocakoğlu, 2012; Tiryakioğlu et al., 2013; Hall et al., 2014; Elitez and Yaltrak, 2014). The regional tectonic meaning of FBFZ is suggested by Barka and Reilinger (1997) that the FBFZ is a major structure separating the western Anatolian extensional province from central Anatolia. The second group of researchers, who are opposed to the FBFZ (ten Veen et al., 2004; 2009; Alçiçek et al., 2006; Koçyiğit and Özacar, 2013; Över et al., 2010; Alçiçek, 2015; Howell et al., 2017; Kaymakçı et al., 2018; Özkaptan et al., 2018; Tosun et al., 2021; Nissen et al., 2022), have generally argued that all the available data show no major earthquake having a pure left-lateral strike-slip focal mechanism solution along the so-called FBFZ and indicate a mix of an uniaxial and radial extension (i.e., Nissen et al., 2022).

Recently, Seyitoğlu et al. (2022b) proposed an alternative view that there are two restraining stepovers between the left-lateral Biruni Fault of the Anatolian Diagonal, the Antalya-Kekova Fault Zone (AKFZ), and the PPSFZ, where the Antalya Thrust / Florence Rise and Fethiye Thrust developed (Figure 1). In this concept, the NE continuation of the PPSFZ in mainland Türkiye is not required, and a structural link of PPSFZ to the Anatolian Diagonal Shear Zone is provided by the AKFZ (Figure 1).

Under these circumstances, the field observations documenting strike-slip faulting in the Bozburun Peninsula presented in this paper contrary to the current active fault map of Emre et al. (2011) are quite significant, because (1) this location can be evaluated as a most northeastern end of the PPSFZ or (2) this location can be evaluated as clear evidence of the on-land continuation of the Ptolemy Fault, Pliny Fault, and Strabo Fault, even though it is located outside of the so-called FBFZ (i.e., Elitez and Yaltrak, 2014).

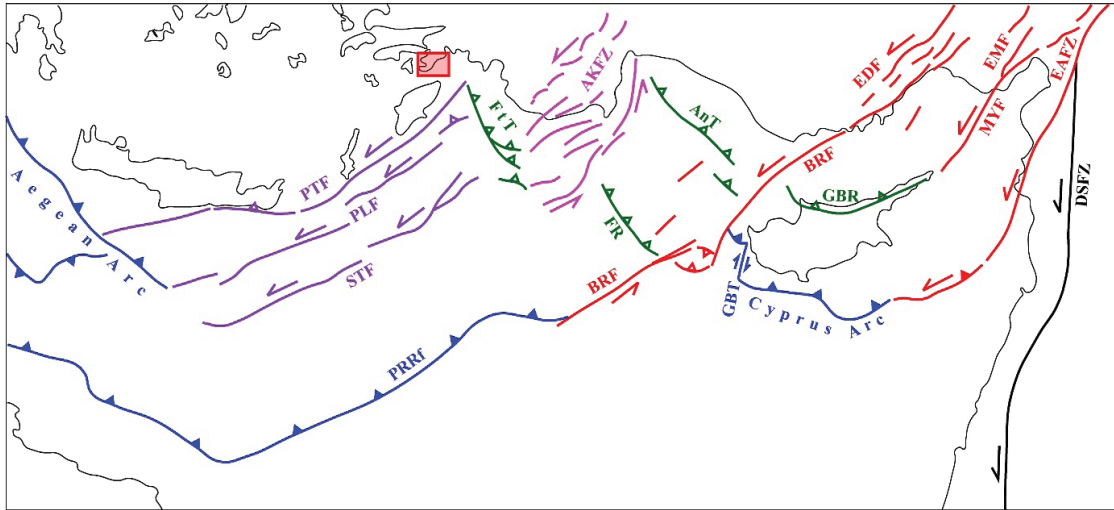


Figure 1. Main neotectonic elements of the eastern Mediterranean and location of Bozburun Peninsula.

AKFZ: Antalya-Kekova Fault Zone, AnT: Antalya Thrust, BRF: Biruni Fault, DSFZ: Dead Sea Fault Zone, EAFZ: East Anatolian Fault Zone, EDF: Ecemiş-Deliler Fault, EMF: Elbistan-Misis Fault, FtT: Fethiye Thrust, FR: Florence Rise, GBT: Gazibaf (Paphos) Transform, GBR: Girne-Besparmak Ridge, MYF: Maraş-Yumurtalık Fault, PLF: Pliny Fault, PRRf: Piri Reis (Mediterranean) Ridge front, PTF: Ptolemy Fault, STF: Strabo Fault, (after Seyitoğlu et al., 2022b).

Şekil 1. Doğu Akdeniz'in başlıca neotektonik unsurları ve Bozburun Yarımadası'nın konumu (Seyitoğlu vd., 2022b'den alınmıştır).

In this paper, we present preliminary strike-slip structural data unrecognized up to now from the Bozburun Peninsula and discuss their implications regarding regional tectonics.

FINDINGS FROM THE BOZBURUN PENINSULA

Current Situation Assessment

The semi-parallel arc shaped normal faults of Selimiye and Bozburun were defined in the Bozburun Peninsula by Emre et al. (2011; 2013) (Figure 2). To the north of Bayırköy, the Selimiye Fault trending in an east-west direction follows a

topographic through; however, north of Selimiye, the same normal fault gains a northeast-southwest direction and follows the coastline of Kepez Dağı. In the footwall of the Selimiye Fault, the Bozburun Fault has the same trend following the northern slopes of Bozcadağ, dipping north and northwest (Figure 2). Further south, the trend of the normal faults turns to northeast-southwest, and the Taşlıca Fault has been drawn as opposite dipping normal fault segments with the Taşlıca settlement in the middle (Figure 2) (Emre et al., 2011). This map of active faulting implies that the Bozburun Peninsula is under extensional tectonics, similar to the rest of western Türkiye (Emre et al., 2013).

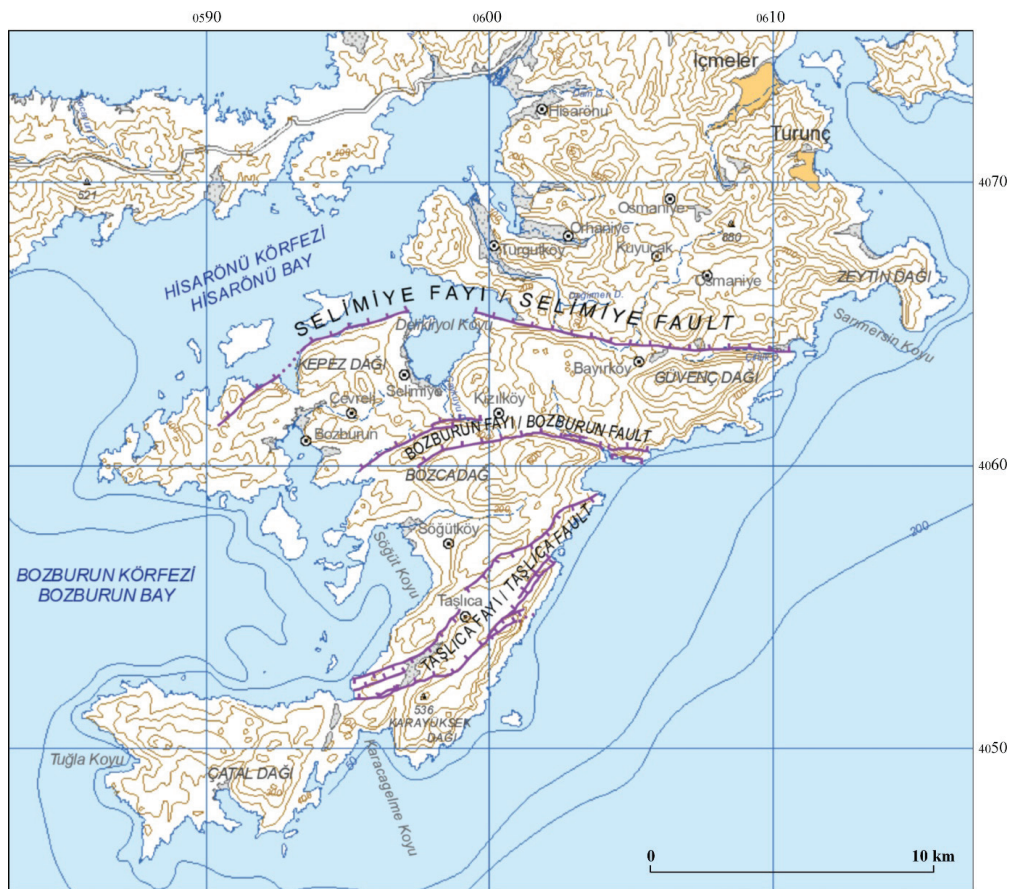


Figure 2. Active fault map of Bozburun Peninsula (Emre et al., 2011).

Şekil 2. Bozburun Yarımadası'nın diri fay haritası (Emre vd., 2011).

Field Observations

The first feature recognized in the field around Bayırköy is the absence of a distinguished topographical difference between the footwall and the hanging wall topography, which would be expected in the so-called active Selimiye normal fault (Figure 2). The structural data obtained from fault surfaces help to characterize two different

strike-slip fault segments (Figure 3a, Table 1); notably, the northeast-southwest trending left-lateral strike-slip Bayır-Çiftlik Fault (BÇF) and the west northwest - east southeast trending right-lateral strike-slip Delikliyol Fault (DYF). These observations are entirely different from the normal faults previously defined by Emre et al. (2011). Therefore, we have applied new fault names in this paper.

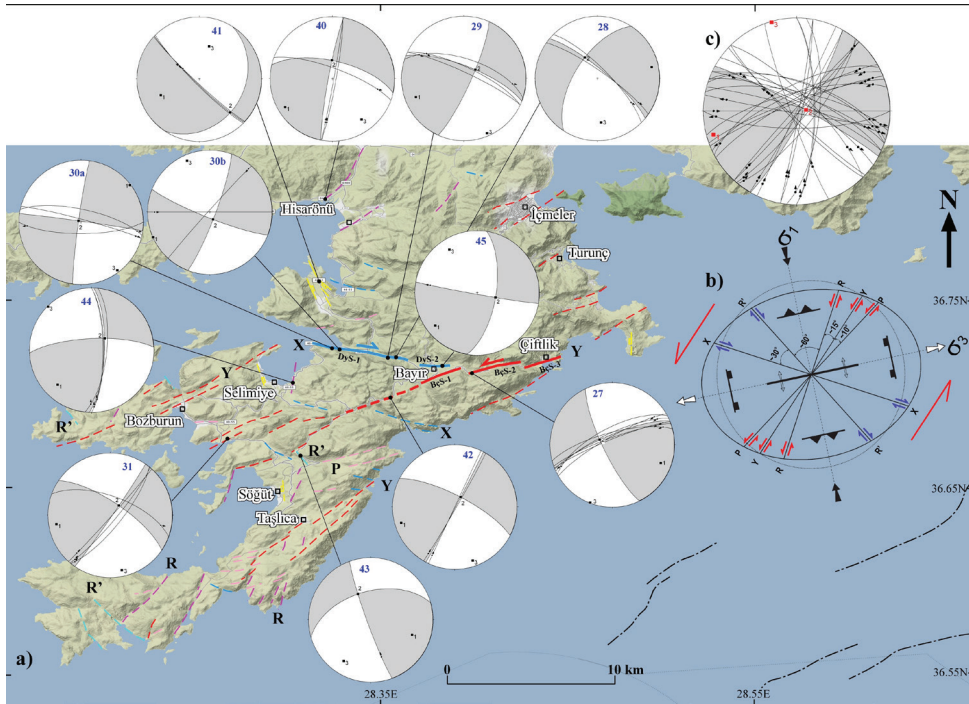


Figure 3. a) Active fault and lineament map of Bozburun Peninsula. BÇS-1, 2, 3 and DyS-1, 2 are segments of BÇF and DYF, respectively. Colored-broken lines are lineaments obtained from Google Earth Images. Black dotted-broken lines are left-lateral faults based on detailed bathymetry in Marmaris Bay (Ocakoğlu, 2012). **b)** The strain ellipse of a left-lateral shear zone and secondary fractures are presented for correlation of faults and lineaments in Bozburun Peninsula. **c)** Overall evaluation of structural data indicating left-lateral shear. Circles represent the equal area lower hemisphere spherical projection of fault planes and slickenlines. Gray (contractional) and white (extensional) areas and circles belong to the fault plane solution obtained by kinematic analysis of the fault data using FaultKin software (Marrett and Allmendinger, 1990; Allmendinger et al., 2012). Number 1, 2, and 3 squares in red indicate the orientation of kinematic (strain) axes. See Table 1 for numerical data.

Şekil 3. a) Bozburun Yarımadası diri fay ve çizgisellik haritası. BÇS-1, 2, 3 ve DyS-1, 2 sırasıyla BÇF ve DYF'nin segmentleridir. Renkli-kesikli çizgiler Google Earth görüntülerinden elde edilen çizgiselliklerdir. Siyah noktalı kesikli çizgiler, Marmaris Körfezi'ndeki detaylı batimetriye dayalı sol yanal faylardır (Ocakoğlu, 2012). **b)** Bozburun Yarımadası'ndaki fayların ve çizgiselliklerin korelasyonu için sunulan bir sol yanal makaslama zonunun yamulma elipsi ve ikincil kırıkları. **c)** Sol yanal makaslama gösteren yapısal verilerin genel değerlendirilmesi. Daireler, fay düzlemleri ve kayma çiziklerinin eşit alan alt yarıküre izdüşümüdür. Gri (daralma) ve beyaz (genişleme) alanları ve çemberler FaultKin yazılımı (Marrett ve Allmendinger, 1990; Allmendinger vd., 2012) kullanılarak elde edilen fay verisinin kinematik analizi sonucu elde edilen fay düzlemi çözümüne aittir. 1, 2 ve 3 kinematik (yamulma) eksenlerinin konumunu göstermektedir. Sayısal veri için Tablo 1'e bakınız.

Table 1. Fault kinematic data obtained from Bozburun Peninsula. Kinematic axes have been determined by using FaultKin software (Marrett and Allmendinger, 1990; Allmendinger et al., 2012). LL: Left lateral, RL: Right lateral, NR: Normal with right lateral component

Çizelge 1. Bozburun Yarımadası'ndan elde edilen fay kinematik verileri. Kinematik eksenler FaultKin yazılımı kullanılarak belirlenmiştir (Marrett ve Allmendinger, 1990; Allmendinger vd., 2012). LL: Sol yanal, RL: Sağ yanal, NR: Sağ yanal bileşenli normal

| # | Latitude (°N) | Longitude (°E) | Field data | | | | | Kinematic (strain) axes | | | | | |
|-----|------------------|-------------------|---------------|------------|--------------|---------------|------|-------------------------|------------|--------------|------------|--------------|------------|
| | | | Fault plane | | Striae | | Slip | S1 | | S2 | | S3 | |
| | | | Strike (°) | Dip (°) | Trend (°) | Plunge (°) | | Trend (°) | Pl. (°) | Trend (°) | Pl. (°) | Trend (°) | Pl. (°) |
| 27 | 36.711549 | 28.198785 | 242 | 68 | 247 | 12 | LL | 111 | 18 | 292 | 72 | 201 | 0 |
| | | | 240 | 80 | 056 | 20 | LL | | | | | | |
| | | | 248 | 83 | 067 | 12 | LL | | | | | | |
| | | | 255 | 74 | 071 | 14 | LL | | | | | | |
| | | | 250 | 81 | 067 | 21 | LL | | | | | | |
| | | | 245 | 75 | 060 | 17 | LL | | | | | | |
| 28 | 36.719853 | 28.157652 | 305 | 80 | 120 | 25 | RL | 078 | 12 | 329 | 58 | 175 | 30 |
| | | | 315 | 76 | 125 | 34 | RL | | | | | | |
| 29 | 36.719899 | 28.154809 | 288 | 64 | 096 | 22 | RL | 249 | 18 | 053 | 71 | 157 | 05 |
| | | | 295 | 75 | 303 | 29 | RL | | | | | | |
| | | | 295 | 82 | 298 | 20 | RL | | | | | | |
| 30a | 36.725049 | 28.125334 | 285 | 86 | 104 | 10 | RL | 053 | 01 | 300 | 86 | 143 | 03 |
| | | | 282 | 73 | 099 | 10 | RL | | | | | | |
| | | | 090 | 75 | 266 | 14 | RL | | | | | | |
| 30b | 36.724753 | 28.128515 | 222 | 88 | 042 | 07 | LL | 246 | 00 | 155 | 79 | 336 | 11 |
| | | | 270 | 90 | 270 | 12 | RL | | | | | | |
| 31 | 36.675029 | 28.068051 | 290 | 65 | 101 | 18 | RL | 260 | 14 | 042 | 73 | 168 | 10 |
| | | | 040 | 82 | 219 | 10 | LL | | | | | | |
| | | | 042 | 88 | 221 | 20 | LL | | | | | | |
| | | | 039 | 75 | 217 | 07 | LL | | | | | | |
| 40 | 36.805386 | 28.121772 | 010 | 85 | 187 | 30 | LL | 239 | 13 | 359 | 65 | 144 | 20 |
| | | | 010 | 88 | 189 | 30 | LL | | | | | | |
| | | | 290 | 76 | 103 | 26 | RL | | | | | | |
| 41 | 36.761246 | 28.118552 | 135 | 83 | 303 | 59 | NR | 247 | 33 | 137 | 27 | 016 | 44 |
| | | | 133 | 85 | 302 | 65 | NR | | | | | | |
| 42 | 36.698907 | 28.157277 | 030 | 88 | 209 | 15 | LL | 253 | 11 | 031 | 75 | 161 | 10 |
| | | | 025 | 90 | 205 | 15 | LL | | | | | | |
| 43 | 36.667362 | 28.107009 | 160 | 85 | 164 | 38 | RL | 110 | 30 | 334 | 52 | 213 | 22 |
| | | | 000 | 74 | 174 | 21 | LL | | | | | | |
| 44 | 36.706046 | 28.103701 | 006 | 70 | 181 | 14 | LL | 224 | 23 | 048 | 67 | 315 | 01 |
| | | | 000 | 75 | 177 | 10 | LL | | | | | | |
| 45 | 36.715314 | 28.186059 | 100 | 88 | 279 | 25 | RL | 232 | 16 | 104 | 65 | 327 | 19 |

The Bayır-Çiftlik Fault (BÇF) has three northeast-southwest trending en-echelon segments (BçS-1_3) (Figure 3a). On the road between Bayır and Çiftlik, the fault surface of BçS-2 is clearly observed. This provides the left-lateral strike-slip structural data (Figure 3a, location 27 and Figure

4). Its continuation toward the northeast presents a flower structure-like fracture style (Figure 5). The shear surfaces providing structural data between Bozburun and Söğüt (Figure 6, location 31) indicate that the segments of BÇF can be securely extended to the southwest.

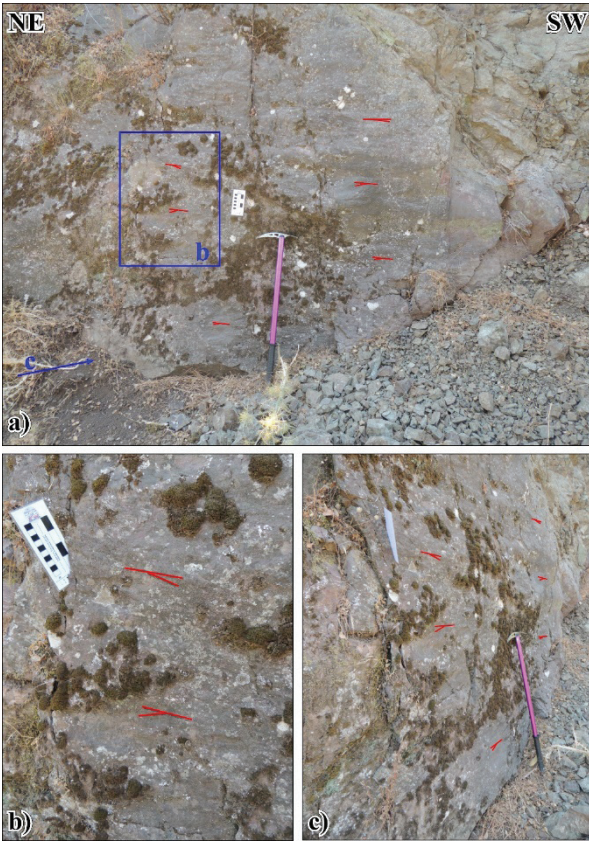


Figure 4. a) Fault surface photo from segment BÇS-2 of Bayır-Çiftlik Fault (BÇF). **b, c)** Details of the fault surface from different angles. Note position of open fractures where the ruler is located, indicating a left-lateral sense of movement. Photos are from location #27 in Figure 3. See Table 1 for numerical data.

Şekil 4. a) Bayır-Çiftlik Fayının (BÇF) BÇS-2 segmentine ait fay düzlemi fotoğrafı. **b, c)** Fay düzleminin farklı açılardan detayları. Cetvelin bulunduğu yer açılma çatlaklarının konumunu ve sol yanıl makaslamayı işaret etmektedir. Fotoğraflar Şekil 3'eki #27 konumundan çekilmiştir. Sayısal veriler için Tablo 1'e bakınız.

The Delikliyol Fault (DYF) has two west northwest – east southeast trending en-echelon segments (DyS-1 and 2) (Figure 3a). The segment-parallel shear surfaces provide right-lateral strike-slip structural data on the road to the west of Bayır (Figure 7).



Figure 5. Field photo of flower structure-like fractures along segment BÇS-2 of Bayır-Çiftlik Fault (BÇF).

Şekil 5. Bayır-Çiftlik Fayı'nın (BÇF) BÇS-2 segmenti boyunca çiçek yapısı benzeri kırıkların arazi fotoğrafı.

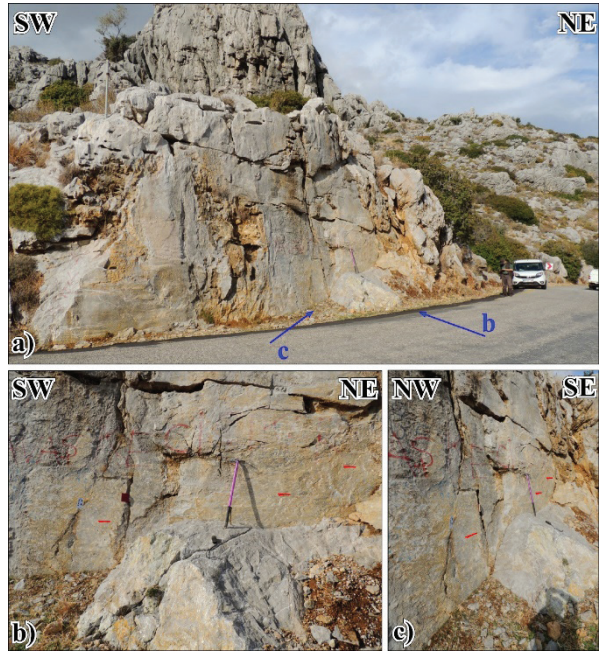


Figure 6. a) Overall view of left-lateral fault surface between Söğüt and Bozburun. **b, c)** Details of fault surfaces from different angles. See position of ruler and field notebook on open fractures to realize left-lateral sense of movement. Photos are from location #31 in Figure 3. See Table 1 for numerical data.

Şekil 6. a) Söğüt-Bozburun arasındaki sol yanıl fay düzleminin genel görünümü. **b, c)** Farklı açılardan fay düzleminin detayları. Sol yanıl hareketin anlaşılması için açılma çatlaklarına yerleştirilen cetvel ve arazi defterinin konumlarına bakınız. Fotoğraflar Şekil 3'eki #31 konumundan çekilmiştir. Sayısal veriler için Tablo 1'e bakınız.



Figure 7. a) Segment DyS-1 of Delikliyol Fault (DYF). **b, c)** Close up views of right-lateral structural data. Photos from location #29 in Figure 3. See Table 1 for numerical data.

Şekil 7. a) Delikliyol Fayının (DYF) DyS-1 segmenti. **b, c)** Sağ yanal yapısal verilerin yakın plan görünüşleri. Fotoğraflar Şekil 3'teki #29 konumundan çekilmiştir. Sayısal veriler için Tablo 1'e bakınız.

The main fault surface of DyS-1 is observed on the south coast of Delikliyol Bay, where the right-lateral strike-slip data were obtained (Figures 3a and 8, locations 30a and 30b). The DyS-2 segment also has a distinct fault scarp showing a right-lateral sense of slip immediately northeast of Bayır (Figure 3a, location 45).

These field observations indicate that the faults are strike-slip in character around Bayır and there is no sign of normal faults creating major topographical differences (Figure 9). It is interesting to see that the north northwest - south southeast trending depression in Turgutköy (see structural data from location 41 in Figure 3a) and stepping topography in Selimiye, Söğüt and east of Çiftlik perfectly fit the position of open fractures /

normal faulting in a left-lateral shear zone (Figure 3b). Moreover, the lineament distribution on the Bozburun Peninsula obtained from Google Earth Images fits well with the secondary fractures (R, R', X and P) that developed in a northeast-southwest trending left-lateral shear zone (Figure 3b), where the BÇF corresponds to the Y-shear and the DYF represents the X-shear (Figure 3a and b). The overall evaluation of structural data obtained from the fault surfaces is also compatible with the northeast-southwest trending left-lateral shear zone (Figure 3c).

SEISMIC ACTIVITY and FOCAL MECHANISM SOLUTIONS

The study region and near vicinity have a high seismicity. A number of earthquakes, both small and moderate, have occurred frequently in the region since the year 1900, and their focal depths have been distributed over a wide range (Figure 10). In Figure 10, the seismic activity having a depth shallower than 30 km around the Bozburun Peninsula is shown in red circles, while the deeper events down to 100 km are represented in yellow.

For the focal mechanism solution, we applied some selection criteria on earthquakes. One of them is the depth of earthquakes. We avoided deeper earthquakes because they could be the result of the subduction of the African plate under the Anatolian plate along the Aegean Arc. Therefore, we generally tried to select crustal earthquakes for the focal mechanism solution. Another criterion is the location of events. We selected only the earthquakes that occurred on the faults we focused on. Our last criterion selected is the quality of seismograms. We tried to use less noisy and nonproblematic waveforms. Besides our own solutions, we also benefited from other focal mechanism solutions calculated by other earthquake observation agencies or researchers. All focal mechanism solutions are listed together with their parameters and beachballs in Table 2.

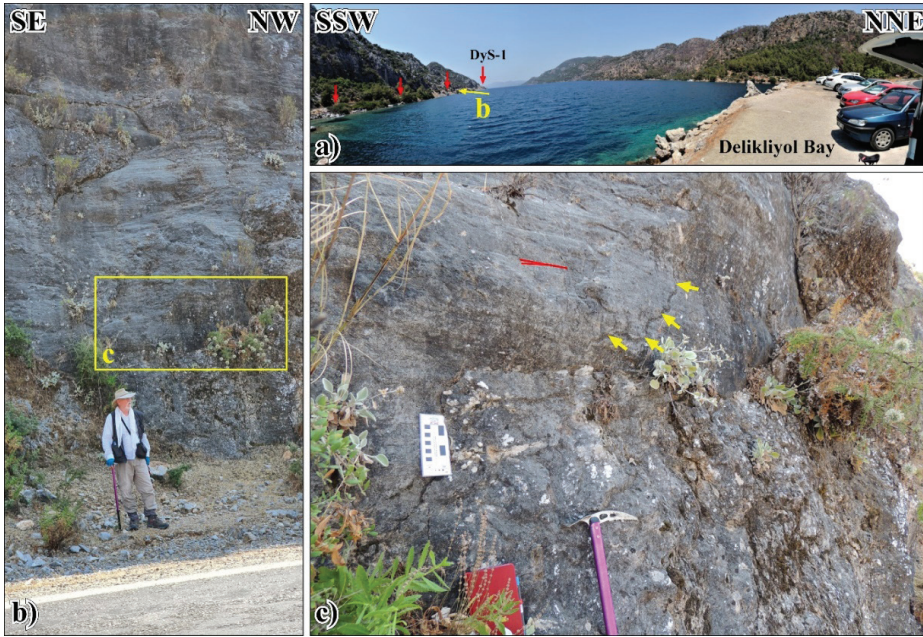


Figure 8. a) Overall position of Delikliyol Fault in Delikliyol Bay. b) Main right-lateral fault surface of segment DyS-1 of Delikliyol Fault (DYF). c) Details of structural data. Note small yellow arrows showing a trace of open fracture indicating right-lateral sense of movement. Photos from location #30a in Figure 3. See Table 1 for numerical data.

Şekil 8. a) Delikliyol Körfezi'ndeki Delikliyol Fayı'nın genel konumu. b) Delikliyol Fayı'nın DyS-1 segmentinin sağ yanıl ana fay yüzeyi. c) Yapısal verilerin detayları. Sağ yanıl hareketin varlığını gösteren açılma çatlaklarının izini gösteren küçük sarı oklara dikkat ediniz. Fotoğraflar Şekil 3'teki #30a konumundan çekilmiştir. Sayısal veriler için Tablo 1'e bakınız.

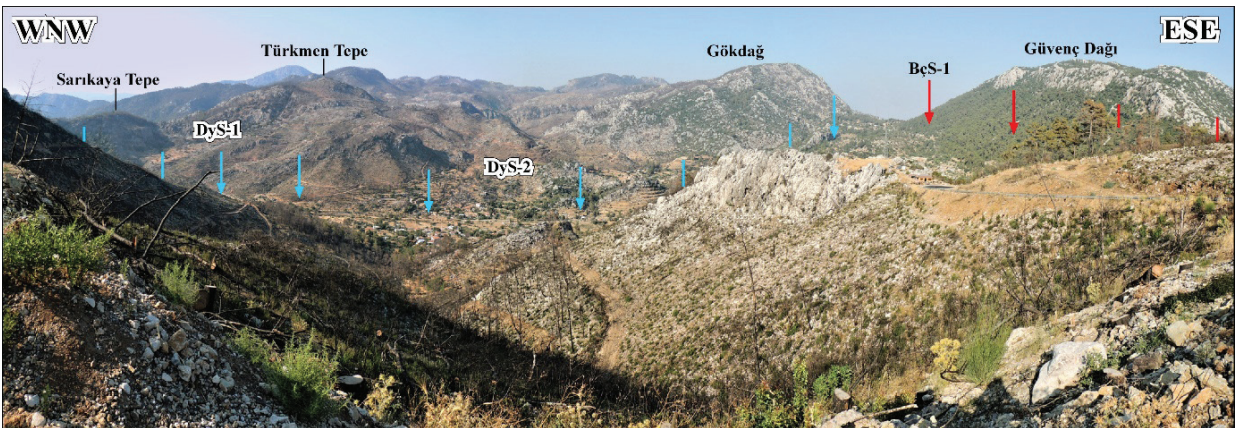


Figure 9. Position of right-lateral segments of Delikliyol Fault (DYF) and left-lateral Bayır-Çiftlik Fault (BÇF) around Bayır after severe forest fire. Note no topographical difference between Gökdağ and Güvenç Dağı, in which Selimiye normal fault is located (Emre et al., 2011, Figure 2).

Şekil 9. Şiddetli bir orman yangını sonrası Delikliyol Fayı'nın (DYF) sağ yanıl segmentleri ile Bayır-Çiftlik Fayı'nın (BÇF) sol yanıl segmentlerinin Bayır çevresindeki konumu. Gökdağ ile Güvenç Dağı arasında konumlandırılan Selimiye normal fayının (Emre vd. 2011, Şekil 2) topoğrafik bir fark yaratmadığına dikkat ediniz.

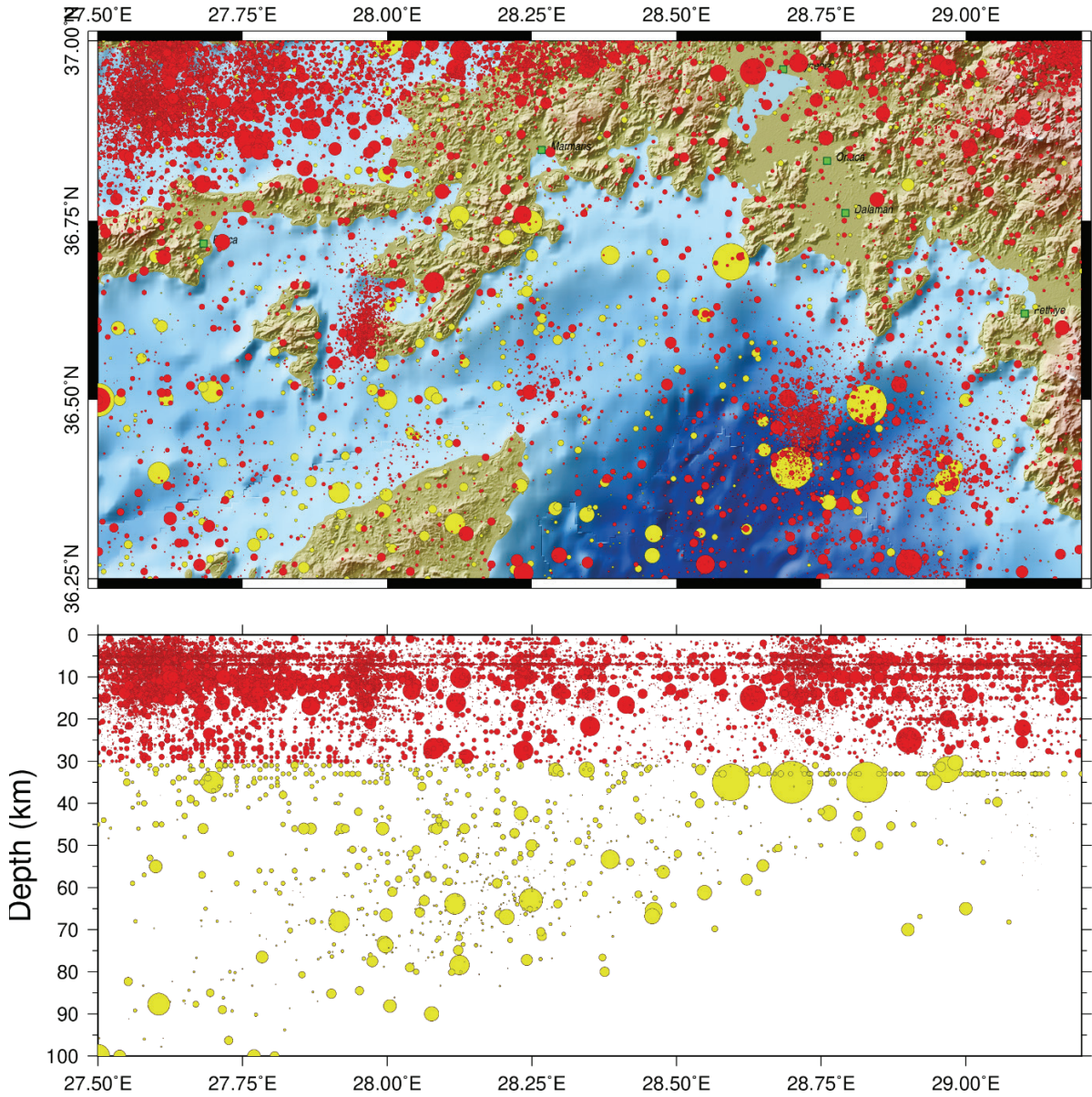


Figure 10. Epicentral (top) and hypocentral (bottom) earthquake distribution around the Bozburun Peninsula and surroundings. Seismicity of the region includes earthquakes that occurred since 1900. Events down to 30 km depth are shown in red circles, deeper events are represented by yellow circles.

Şekil 10. Bozburun Yarımadası ve çevresinde dış merkez (üstte) ve iç merkez (alt) deprem dağılımı. Bölgenin depremselliği 1900'den beri meydana gelen depremleri içermektedir. 30 km derinliğe kadar olan sismik etkinlik kırmızı renkli daireler ile, daha derin olan etkinlik sarı daireler ile temsil edilmektedir.

Table 2. Earthquake focal parameters and focal mechanism solutions of the selected seismic events around Bozburun Peninsula.**Çizelge 2.** Bozburun Yarımadası çevresinde seçilen sismik olayların deprem odak parametreleri ve odak mekanizması çözümleri.




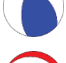
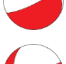

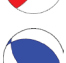






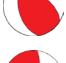










| ID | Earthquake focal parameters | | | | | | | | Focal mechanism solutions | | | | | | | |
|----|-----------------------------|--------------------|-----------|-----------|------------|------|------|-------|---------------------------|----------|-----------|----------|----------|-----------|---|---------|
| | Date (y.m.d) | Time (GMT) (h:m:s) | Lat. (°N) | Lon. (°E) | Depth (km) | Mag. | MTyp | Ref | Str1 (°) | Dip1 (°) | Rake1 (°) | Str2 (°) | Dip2 (°) | Rake2 (°) | Beach ball | Ref |
| 1 | 1999.10.05 | 00:53:29 | 36.7390 | 28.2260 | 19 | 5.2 | Mw | K-17 | 4 | 83 | 171 | 95 | 81 | 7 |  | ISC |
| 2 | 2002.09.26 | 20:44:07 | 36.6670 | 28.0280 | 18 | 4.4 | Mw | ISC | 70 | 57 | -95 | 259 | 33 | -82 |  | ZUR-RMT |
| 3 | 2009.12.30 | 11:00:51 | 36.6435 | 27.9160 | 12 | 3.6 | Mw | KOERI | 73 | 76 | -104 | 300 | 20 | -45 |  | TS |
| 4 | 2010.04.28 | 16:35:08 | 36.3285 | 27.6806 | 16.8 | 4.4 | Mw | K-17 | 191 | 60 | 132 | 310 | 50 | 40 |  | ISC |
| 5 | 2010.08.08 | 02:12:05 | 36.6545 | 27.9605 | 14 | 3.2 | Mw | KOERI | 63 | 77 | -106 | 295 | 20 | -40 |  | TS |
| 6 | 2011.01.12 | 03:04:03 | 36.8787 | 28.0757 | 12 | 3.8 | Mw | KOERI | 65 | 90 | -50 | 155 | 40 | -180 |  | TS |
| 7 | 2011.04.23 | 03:04:14 | 36.6978 | 28.4397 | 19 | 3.5 | Mw | KOERI | 302 | 80 | 165 | 35 | 75 | 10 |  | TS |
| 8 | 2012.06.10 | 09:49:36 | 36.4762 | 28.9295 | 26.85 | 5.0 | Ml | AFAD | 133 | 51 | 101 | 295 | 40 | 76 |  | AFAD |
| 9 | 2012.06.10 | 15:28:32 | 36.4737 | 28.9608 | 28.64 | 4.5 | Ml | AFAD | 163 | 79 | 174 | 254 | 84 | 11 |  | AFAD |
| 10 | 2012.06.11 | 02:06:34 | 36.4258 | 28.9788 | 28.19 | 4.4 | Ml | AFAD | 220 | 81 | -5 | 311 | 85 | -171 |  | AFAD |
| 11 | 2012.06.11 | 14:00:17 | 36.4267 | 29.0053 | 28.69 | 4.0 | Ml | AFAD | 295 | 62 | -171 | 201 | 82 | -28 |  | AFAD |
| 12 | 2012.06.11 | 16:35:37 | 36.4112 | 28.9907 | 27.94 | 4.4 | Ml | AFAD | 225 | 73 | -6 | 317 | 84 | -163 |  | AFAD |
| 13 | 2012.06.11 | 19:51:06 | 36.4575 | 28.9837 | 27.87 | 4.3 | Ml | AFAD | 300 | 44 | -117 | 156 | 52 | -66 |  | AFAD |
| 14 | 2012.06.12 | 21:58:12 | 36.4578 | 28.9283 | 28.02 | 4.5 | Ml | AFAD | 138 | 44 | -162 | 35 | 78 | -46 |  | AFAD |
| 15 | 2012.10.20 | 01:09:39 | 36.5000 | 28.2223 | 8 | 3.9 | Mw | KOERI | 300 | 55 | 55 | 171 | 48 | 129 |  | TS |
| 16 | 2012.11.09 | 04:46:14 | 36.6151 | 27.9547 | 15 | 3.8 | Mw | KOERI | 7 | 75 | 138 | 110 | 50 | 20 |  | TS |
| 17 | 2012.11.24 | 21:04:18 | 36.5520 | 27.9087 | 10 | 4.1 | Mw | KOERI | 179 | 86 | -135 | 85 | 45 | -5 |  | TS |
| 18 | 2012.11.24 | 21:35:22 | 36.5945 | 27.9312 | 12 | 3.8 | Mw | KOERI | 205 | 59 | -106 | 55 | 35 | -65 |  | TS |

Table 2. *Continued.*

Çizelge 2. Devam

| ID | Earthquake focal parameters | | | | | | | | Focal mechanism solutions | | | | | | | |
|----|-----------------------------|--------------------|-----------|-----------|------------|------|------|-------|---------------------------|----------|-----------|----------|----------|-----------|---|------|
| | Date (y.m.d) | Time (GMT) (h:m:s) | Lat. (°N) | Lon. (°E) | Depth (km) | Mag. | MTyp | Ref | Str1 (°) | Dip1 (°) | Rake1 (°) | Str2 (°) | Dip2 (°) | Rake2 (°) | Beach ball | Ref |
| 19 | 2012.11.25 | 08:51:46 | 36.6322 | 27.9113 | 12 | 3.9 | Mw | KOERI | 337 | 57 | 130 | 100 | 50 | 45 |  | TS |
| 20 | 2012.11.26 | 17:35:42 | 36.6038 | 27.9572 | 12 | 4.6 | Mw | KOERI | 204 | 64 | -114 | 70 | 35 | -50 |  | TS |
| 21 | 2012.11.26 | 21:20:33 | 36.6383 | 27.9588 | 11 | 3.4 | Mw | KOERI | 211 | 76 | -122 | 100 | 35 | -25 |  | TS |
| 22 | 2012.12.02 | 19:02:58 | 36.6298 | 27.9543 | 4.1 | 3.5 | Mw | K-17 | 299 | 35 | -163 | 195 | 80 | -57 |  | AFAD |
| 23 | 2013.01.11 | 10:28:23 | 36.5983 | 27.9288 | 12 | 3.7 | Mw | KOERI | 226 | 63 | -127 | 105 | 45 | -40 |  | TS |
| 24 | 2019.10.03 | 04:44:55 | 36.3147 | 28.5437 | 20 | 5.1 | Mw | KOERI | 210 | 65 | 70 | 71 | 32 | 126 |  | TS |

AFAD: Disaster and Emergency Management Authority; ISC: International Seismological Centre; K-17: Kılıç et al. (2017); KOERI: Kandilli Observatory and Earthquake Research Institute; LDEO: Lamont-Doherty Earth Observatory; TS: This Study; ZUR-RTM: Zurich Moment Tensors, Swiss Seismological Service.

To derive the focal mechanism solutions for the selected events, we used the moment tensor inversion method. We utilized the algorithm found in ‘Computer Programs in Seismology’ by Herrmann (2013) for Regional Moment Tensor (RMT) inversion, which involves fitting synthetic waveforms to the observed data. We retrieved three-component broadband waveform data for the RMT solutions from the European Integrated Data Archive Service (<http://www.orfeus-eu.org/data/eida>) and the Turkish Earthquake Data Center System (TEDCS) of the Emergency Management Presidency (AFAD). We used the waveform data only from the stations up to 700 km epicentral distance.

For the inversion, both the observed and synthetic Green’s function waveforms were cut from a range of 5–10 s before the P-wave’s first-arrival to a range of 110–180 s after it. During the inversion steps, a three-pole causal Butterworth bandpass filter with a 0.02–0.10 Hz band range was used for the events. Generally, the 0.06-0.08

Hz bandpass filter range was preferred for the most of the data. Furthermore, an optional microseism rejection filter was applied to enhance the signal-to-noise ratio when needed. During the moment tensor inversion process, we removed components having noisy and problematic signals.

The three largest earthquakes around the Bozburun Peninsula shallower than 30 km were #1_1999.10.05 (Mw=5.2), #8_2012.06.10 (Ml=5.0), and #24_2019.10.03 (Mw=5.1) (Table 2). The seismic activity created a cluster of 10 focal mechanism solutions between Sömbeki (Simi) island and the Bozburun Peninsula, indicating dominantly normal faulting. However, the #7_2011.04.23 (Mw= 3.5) earthquake located 18 km east, southeast of Çiftlik, provides a focal mechanism solution that is highly compatible with the left-lateral strike-slip structural data obtained from fault surfaces similar to the aftershocks of the #8_2012.06.10 (Ml=5.0) earthquake in the Fethiye Gulf (Figure 11).

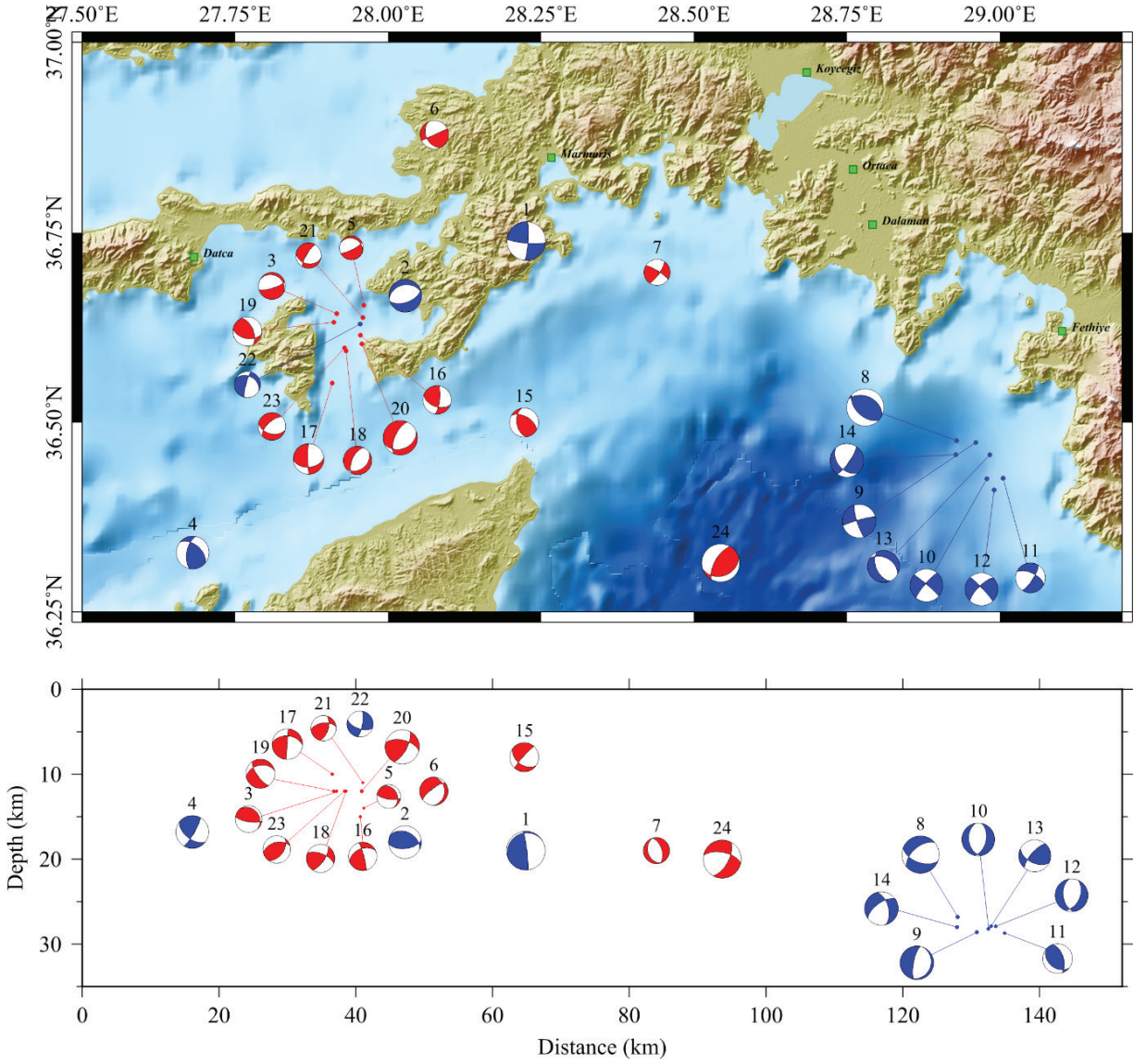


Figure 11. Available focal mechanism solutions of earthquakes shallower than 30 km depth around the Bozburun Peninsula. Surroundings are shown both as map view and vertical section along a latitude. Size of beachballs is proportional to earthquake magnitudes. See Table 2 for details and references.

Şekil 11. Bozburun Yarımadası ve çevresinde 30 km'den daha sığ olan depremlerin mevcut odak mekanizması çözümleri hem harita görünümünde hem de bir enlem boyunca dikey kesitte gösterilmiştir. Odak mekanizma çözümlerinin boyutu, deprem büyüklükleriyle orantılıdır. Ayrıntılar ve referanslar için Tablo 2'ye bakınız.

DISCUSSION

The overall evaluation of the structural data obtained from fault surfaces in the Bozburun Peninsula indicates northeast-southwest trending left-lateral strike-slip faulting (Figures 3b and 12a),

which is not compatible with the active normal faults previously indicated on the Active Fault Map of Turkey (Emre et al., 2011). Moreover, the overall evaluation of focal mechanism solutions around the Bozburun Peninsula also indicates

a left-lateral strike-slip tectonic setting (Figure 12b). When we combined structural data from the field and focal mechanism solutions (Figure 12c), it is clearly seen that the Bozburun Peninsula is under the influence of the left-lateral Ptolemy-Pliny-Strabo Fault Zone (PPSFZ). This is the first structural data in the Turkish mainland showing the influence of PPSFZ. On the other hand, as briefly summarized in the Introduction section, there is no convincing data regarding the northeast continuation of the left-lateral shear zone, which has been named as the Fethiye-Burdur Fault Zone. An alternative suggestion is proposed that the PPSFZ creates a restraining stepover with the Antalya-Kekova Fault Zone, where the Fethiye Thrust is developed in the northern margin of the Rhodos basin (Seyitoğlu et al., 2022b).

In the north of the Bozburun Peninsula, however, an entirely different extensional active tectonic regime is evidenced by intense seismicity providing mainly normal fault-related focal mechanism solutions around the Gökova Gulf (Ocakoğlu et al., 2018; Dikbaş et al., 2022; Tanülkü et al., 2022).

CONCLUSION

In the Bozburun Peninsula, our field observations providing structural data from exposed fault surfaces indicate that the active tectonic style is strike-slip in nature. The segments of the left-lateral strike-slip Bayır-Çiftlik Fault (BÇF) and the right-lateral Delikliyol Fault (DYF) were determined. The lineament distribution using Google Earth Images and the focal mechanism solutions for the earthquakes in the vicinity of the Bozburun Peninsula show that the BÇF is Y-shear and the DYF represents X-shear in a northeast-southwest trending left-lateral shear zone. It can be concluded that the Bozburun Peninsula is located on the northeastern tip of the Ptolemy-Pliny-Strabo Fault Zone.

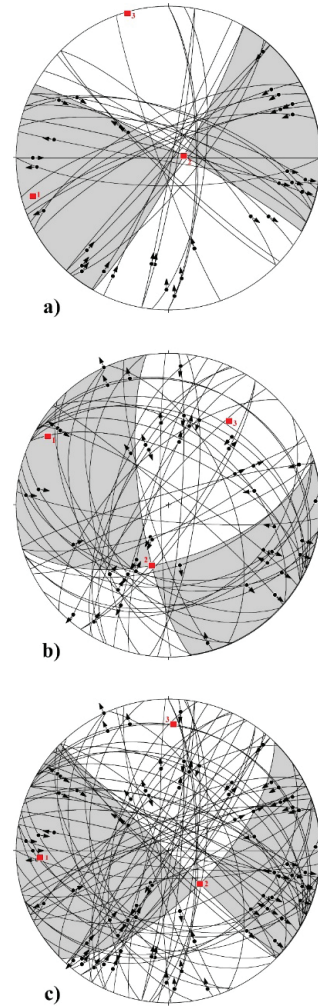


Figure 12. **a)** Structural data from fault surfaces (32 fault planes) measured in the field from Bozburun Peninsula. See Table 1 for numerical data. **b)** Structural data obtained from focal mechanism solutions (45 fault planes) around Bozburun Peninsula. See Table 2 for details. **c)** Overall evaluation of structural data, both field observations and focal mechanism solutions, indicating that Bozburun Peninsula is under the influence of the left-lateral Ptolemy-Pliny-Strabo Shear Zone. The stereonets are equal area lower hemisphere spherical projection of fault planes and slickenlines. Gray (contractional) and white (extensional) areas and circles belong to the fault plane solution obtained by kinematic analysis of the fault data using FaultKin software (Marrett and Allmendinger, 1990; Allmendinger et al., 2012). Numbers 1, 2, and 3 in red indicate orientation of kinematic (strain) axes.

Şekil 12. **a)** Bozburun Yarımadası'ndan arazide ölçülen fay yüzeylerinden (32 fay düzlemi) yapısal veriler. Sayısal veriler için Tablo 1'e bakınız. **b)**

Bozburun Yarımadası çevresindeki odak mekanizması çözümlerinden (45 fay düzlemi) elde edilen yapısal veriler. Ayrıntılar için Tablo 2'ye bakınız. c) Bozburun Yarımadası'nın sol-yanal Ptolemy-Pliny-Strabo Makaslama Zonu'nun etkisi altında olduğunu gösteren hem saha gözlemleri hem de odak mekanizması çözümlerine ait yapısal verilerin genel değerlendirmesi. Stereonetler, fay düzlemlerinin ve kayma çiziklerinin eşit alan alt yarımküre izdüşümüdür. Gri (daralma) ve beyaz (genişleme) alanlar ve daireler, fay verilerinin FaultKin yazılımı kullanılarak kinematik analizi ile elde edilen fay düzlemi çözümüne aittir (Marrett ve Allmendinger, 1990; Allmendinger vd., 2012). 1, 2 ve 3, kinematik (yamulma) eksenlerinin yönünü gösterir.

GENİŞLETİLMİŞ ÖZET

Levha tektoniğinin başlangıç döneminde varlığı fark edilen Ege Yayı, doğu kenarında Yay'a paralel doğrultu atımlı karaktere sahiptir (McKenzie, 1970; 1972; Papazachos ve Comninakis, 1971; Dewey vd., 1973; Le Pichon ve Angelier, 1979; Taymaz vd., 1990). Günümüzde Ptolemy-Pliny-Strabo Fay Zonu olarak anılmakta olan (Shaw ve Jackson, 2010; Özbakır vd., 2013) yapı üzerinde GPS temelli blok modelleme çalışmalarına göre sol yanallı kayma oranı saptanmıştır (Reilinger vd., 2006; 2010; $49,5 \pm 0,4$ mm/yıl; Seyitoğlu vd., 2022a; $37,3 \pm 0,4$ mm/yıl) ve dalmakta olan Afrika levhasındaki aktif yırtılmanın yüzeydeki ifadesi olarak değerlendirilmektedir (Özbakır vd., 2013).

Bölgedeki temel tartışmalardan birini Ptolemy-Pliny-Strabo Fay Zonu'nun Türkiye ana karasındaki devamlılığı oluşturmaktadır. Bazı araştırmacılara göre bu devamlılık Fethiye-Burdur Fay Zonu tarafından sağlanmaktadır (Barka ve Reilinger, 1997; Ocağolu, 2012; Tiryakioğlu vd., 2013; Hall vd., 2014; Elitez ve Yaltrak, 2014). Diğer araştırmacı grubu ise bu zon içinde depremlere ait saf sol yanallı odak mekanizması çözümü elde edilemediği ve çok yönlü genişlemeyi işaret eden çözümlerin bulunduğu gerekçesi ile Fethiye-Burdur Fay Zonu'nun varlığını sorgulamaktadır (ten Veen vd., 2004; 2009; Alçiçek vd., 2006; Koçyiğit ve Özacar, 2013; Över vd., 2010; Alçiçek, 2015; Howell vd., 2017; Kaymakçı vd., 2018; Özkaptan vd., 2018; Tosun vd. 2021; Nissen vd., 2022). Yakın zamanda






yayınlanan çalışmaya göre ise (örn., Seyitoğlu vd., 2022b) Ptolemy-Pliny-Strabo Fay Zonu, Antalya-Kekova Fay Zonu ve Anadolu Çaprazı'nın Biruni Fayı daralmalı sıçramalar oluşturmakta ve Anadolu Levhasının GB'ya hareketi tartışmalı Fethiye-Burdur Fay Zonu gibi bir yapıya ihtiyaç kalmadan bu sistemle karşılanmaktadır (Şekil 1).

Türkiye ana karasının güneybatı ucunu oluşturan Bozburun Yarımadası Ptolemy-Pliny-Strabo Fay Zonu'na en yakın konumdadır (Şekil 1). Mevcut diri fay haritasında yarımada üzerinde D-B ve KD-GB yönlü normal faylar gösterilmiştir (Emre vd. 2011) (Şekil 2). Ancak arazi çalışmalarımızda fay düzlemleri üzerinden elde edilen kayma çizikleri sayesinde sağ ve sol yanallı doğrultu atımlı fay segmentleri saptanmıştır (Şekil 3 ve 9). Mevcut diri fay haritası ile uyumsuz olan bu durum, yüksek çözünürlüklü uydu görüntülerinden elde edilen çizgiselliklerin yorumlanması ile test edilmiş ve Bozburun Yarımadası'nın KD-GB sol yanallı makaslamanın etkisinde olduğu sonucuna varılmıştır. Bu yapısal değerlendirmenin diri faylanma ile ilişkisini kurabilmek için yarımada çevresinde meydana gelen 30 km'den daha sığ sismik etkinlik incelenerek odak mekanizma çözümleri elde edilmiştir (Şekil 10 ve 11). Arazi gözlemlerinden elde edilen yapısal verilerle odak mekanizmalarından elde edilen verilerin genel değerlendirmesi sol yanallı makaslama zonunun varlığına işaret etmektedir (Şekil 12). Sonuç olarak, Bozburun yarımadasında saptanan sol yanallı makaslama, Ptolemy-Pliny-Strabo Fay Zonu'nun en KD ucunu temsil ediyor olmalıdır.

ACKNOWLEDGEMENTS

This paper is a part of a project entitled "Investigation of the deep seismic velocity structure of the Gulf of Gökova and surroundings by tomographic methods and associating with tectonic structures in the region (UDAP-Ç-19-20)", supported by AFAD. We are grateful to the referees for their constructive comments that improved the earlier version of the manuscript.

ORCID

Gürol Seyitoğlu  <https://orcid.org/0000-0001-7993-898X>
Bülent Kaypak  <https://orcid.org/0000-0003-4650-9171>
Edanur Tanülkü  <https://orcid.org/0000-0001-7353-7261>
Tolga Karabyıkođlu  <https://orcid.org/0000-0001-8862-7526>
Begüm Koca  <https://orcid.org/0000-0002-4226-0244>

REFERENCES

- Alçıçek, M. C. (2015). Comment on “The Fethiye-Burdur Fault Zone: a component of upper plate extension of the subduction edge propagator fault linking Hellenic and Cyprus Arcs, Eastern Mediterranean. *Tectonophysics*, 635, 80-99.
- Alçıçek, M. C., ten Veen J.H. & Özkul, M. (2006). Neotectonic development of the Çameli Basin, southwestern Anatolia, Turkey. *Geological Society Special Publication*, 260, 591-611.
- Allmendinger, R. W., Cardozo, N. C. & Fisher, D. (2012). *Structural Geology Algorithms: Vectors and Tensors*. Cambridge University Press, 289 p.
- Barka, A. & Reilinger, R. (1997). Active tectonics of the Eastern Mediterranean region: deduced from GPS, neotectonic and seismicity data. *Annali Di Geofisica*, XL, 587-610.
- Dewey, J. F., Pitman III, W. C., Ryan, W. B. F. & Bonnin, J. (1973). Plate Tectonics and the evolution of the Alpine system. *Geological Society of America Bulletin*, 84, 3137-3180.
- Dikbaş, A., Akyüz, H.S., Basmenji, M. & Kırkan, E. (2022). Earthquake history of the Gökova fault zone by paleoseismologic trenching, SW Turkey. *Natural Hazards*, 112, 2695-2716. <https://doi.org/10.1007/s11069-022-05284-0>
- Elitez, İ. & Yaltrak, C. (2014). Miocene-Quaternary geodynamics of Çameli Basin, Burdur-Fethiye Shear Zone (SW Turkey). *Geological Bulletin of Turkey*, 57(3) 41-67. <https://doi.org/10.25288/tjb.298714>
- Emre, Ö., Duman, T. Y. & Özalp, S. (2011). *1:250,000 Scale Active Fault Map Series of Turkey, Marmaris (NJ35-15) Quadrangle*. Serial Number 8, General Directorate of Mineral Research and Exploration, Ankara-Türkiye.
- Emre, Ö., Duman, T. Y., Özalp, S., Elmacı, H., Olgun, Ş. & Şarođlu, F. (2013). *Active Fault Map of Turkey with an Explanatory Text 1:1,250,000 scale*. General Directorate of Mineral Research and Exploration, Special Publication Series 30.
- Hall, J., Aksu, A.E., Elitez, İ., Yaltrak, C. & Çifçi, G. (2014). The Fethiye - Burdur Fault Zone: A component of upper plate extension of the subduction transform edge propagator fault linking Hellenic and Cyprus Arcs, Eastern Mediterranean. *Tectonophysics*, 635, 80-99. <https://doi.org/10.1016/j.tecto.2014.05.002>
- Herrmann, R. B. (2013). Computer programs in seismology: An evolving tool for instruction and research. *Seismological Research Letters*, 84, 1081-1088. <https://doi.org/10.1785/0220110096>
- Howell, A., Jackson, J., Copley, A., McKenzie, D. & Nissen, E. (2017). Subduction and vertical coastal motions in the eastern Mediterranean. *Geophysical Journal International*, 211(1), 593-620. <https://doi.org/10.1093/gji/ggx307>
- Kaymakçı, N., Langereis, C., Özkaptan, M., Özacar, A. A., Gülyüz, E., Uzel, B. & Sözbilir, H. (2018). Paleomagnetic evidence for upper plate response to a STEP fault, SW Anatolia. *Earth and Planetary Science Letters*, 498, 101-115. <https://doi.org/10.1016/j.epsl.2018.06.022>
- Kılıç, T., Kartal, R. F., Kadiriođlu, F. T., Duman, T. Y. & Özalp, S. (2017). Türkiye ve yakın çevresi için düzenlenmiş moment tensor (1906-2012) katalođu Mw=4,0). T. Y. Duman (Ed.), *Türkiye Sismotektonik Haritası, Özel Yayınlar Serisi-34*, Maden Tetkik ve Arama Genel Müdürlüğü, Ankara-Türkiye.
- Koçyiđit, A. & Özacar, A. (2003). Extensional neotectonics regime through the NE edge of the outer Isparta angle, SW Turkey: New field and seismic data. *Turkish Journal of Earth Sciences*, 12, 67-90.
- Le Pichon, X. & Angelier, J. (1979). The Hellenic Arc and Trench System: A key to the Neotectonic evolution of the Eastern Mediterranean Area. *Tectonophysics*, 60, 1-42.
- Marrett, R. & Allmendinger, R. W. (1990). Kinematic analysis of fault-slip data. *Journal of Structural Geology*, 12, 973-986.
- McKenzie, D. (1970). Plate Tectonics of the Mediterranean Region. *Nature*, 226, 239-243.
- McKenzie, D. (1972). Active Tectonics of the Mediterranean Region. *Geophysical Journal of the Royal Astronomical Society*, 30, 109-185.
- Nissen, E., Cambaz, M. D., Gaudreau, E., Howell, A., Karasözen, E. & Savidge, E. (2022). A reappraisal of active tectonics along the Fethiye - Burdur trend, southwestern Turkey. *Geophysical Journal International*, 230(2), 1030-1051. <https://doi.org/10.1093/gji/ggac096>

- Ocakoğlu, N. (2012). Investigation of Fethiye-Marmaris Bay (SW Anatolia): seismic and morphologic evidences from the missing link between the Pliny Trench and the Fethiye-Burdur Fault Zone. *Geo-Marine Letters*, 32, 17-28. <https://doi.org/10.1007/s00367-011-0234-2>
- Ocakoğlu, N., Nomikou, P., İşcan, Y., Loreto, M.F. & Lampridou, D. (2018). Evidence of extensional and strike-slip deformation in the offshore Gökova-Kos area affected by the July 2017 MW6.6 Bodrum-Kos earthquake, eastern Aegean Sea. *Geo-Marine Letters*, 38, 211-225. <https://doi.org/10.1007/s00367-017-0532-4>
- Över, S., Pınar, A., Özden, S., Yılmaz, H., Ünlügenç, U. C. & Kamacı, Z. (2010). Late Cenozoic stress field in the Çameli basin, SW Turkey. *Tectonophysics*, 492, 60-72.
- Özbakır, A. D., Şengör, A. M. C., Wortel, M. J. R. & Govers, R. (2013). The Pliny-Strabo trench region: A large shear zone resulting from slab tearing. *Earth and Planetary Science Letters*, 375, 188-195.
- Özkaptan, M., Kaymakçı, N., Langereis, C. G., Gülyüz, E., Özacar, A. A., Uzel, B. & Sözbilir, H. (2018). Age and kinematics of the Burdur Basin: inferences for existence of the Fethiye - Burdur Fault Zone in SW Anatolia (Turkey). *Tectonophysics*, 744, 256-274. <https://doi.org/10.1016/j.tecto.2018.07.009>
- Papazachos, B. C. & Comninakis, P. E. (1971). Geophysical and tectonic features of the Aegean Arc. *Journal of Geophysical Research*, 76, 8517-8533.
- Reilinger, R., McClusky, S., Paradissis, D., Ergintav, S., Vernant, P. (2010). Geodetic constraints on the tectonic evolution of the Aegean region and strain accumulation along the Hellenic subduction zone. *Tectonophysics*, 488, 22-30.
- Reilinger, R., McClusky, S., Vernant, P., Lawrence, S., Ergintav, S., Çakmak, R., ... Karam, G. (2006). GPS constraints on continental deformation in the Africa - Arabia-Eurasia continental collision zone and implications for the dynamics of plate interactions. *Journal of Geophysical Research*, 111(B5), Article B05411. <https://doi.org/10.1029/2005JB004051>
- Seyitoğlu, G., Aktuğ, B., Esat, K. & Kaypak, B. (2022a). Neotectonics of Turkey (Türkiye) and surrounding regions: a new perspective with block modelling. *Geologica Acta*, 20, 1-21. <https://doi.org/10.1344/GeologicaActa2022.20.4>
- Seyitoğlu, G., Tunçel, E., Kaypak, B., Esat, K. & Gökkaya, E. (2022b). The Anatolian Diagonal: a broad left-lateral shear zone between the North Anatolian Fault Zone and the Aegean/Cyprus Arcs. *Geological Bulletin of Turkey*, 65(2), 93-116. <https://doi.org/10.25288/tjb.1015537>
- Shaw, B. & Jackson, J. (2010). Earthquake mechanisms and active tectonics of the Hellenic subduction zone. *Geophysical Journal International*, 81, 966-984.
- Tanülkü, E., Güvenli, B., Bilgiç, T., Koca, B. & Kaypak, B. (2022). *Source parameters of the Gulf of Gökova and surrounding earthquakes*. In K. Esat & S. Akiska (Eds.), 74th Geological Congress of Turkey, Abstracts Book (pp.: 399). Chamber of Geological Engineers of Turkey Publications, Ankara.
- Taymaz, T., Jackson, J. & Westaway, R. (1990). Earthquake mechanisms in the Hellenic Trench near Crete. *Geophysical Journal International*, 102, 695-731.
- ten Veen, J. H., Woodside, J. M., Zitter, T. A. C., Dumont, J. F., Mascle, J. & Volkonskaia, A. (2004). Neotectonic evolution of the Anaximander Mountains at the junction of the Hellenic and Cyprus arcs. *Tectonophysics*, 391, 35-65.
- ten Veen, J. H., Boulton, S. J. & Alçiçek, M. C. (2009). From palaeotectonics to neotectonics in the Neotethys realm: The importance of kinematic decoupling and inherited structural grain in SW Anatolia (Turkey). *Tectonophysics*, 473, 261-281.
- Tiryakioğlu, İ., Floyd, M., Erdoğan, S., Gülal, E., Ergintav, S., McClusky, S. & Reilinger, R. (2013). GPS Constraints on active deformation in the Isparta Angle region of SW Turkey. *Geophysical Journal International*, 195(3), 1455-1463. <https://doi.org/10.1093/gji/ggt323>
- Tosun, L., Avşar, U., Avşar, Ö., Dondurur, D. & Kaymakçı, N. (2021). Active tectonics and kinematics of Fethiye – Göcek Bay, SW Turkey: Insight about the eastern edge of Pliny-Strabo Trenches. *Journal of Structural Geology*, 145, Article 104287. <https://doi.org/10.1016/j.jsg.2021.104287>